

000
001
002054
055
056

Supplementary Materials for “Unfolding Framework with Prior of Convolution-Transformer Mixture and Uncertainty Estimation for Video Snapshot Compressive Imaging”

057
058
059003
004
005
006
007060
061
062008
009
010
011063
064
065012
013
014066
067
068

Abstract

In this supplementary material, we provide the details of network structure, comparison of different algorithms’ adaptability and full original results of both simulation and real experiments (in the .Zip file).

1. Details of Network Design

Assume x to be the input feature of each phase. x is first fed into 3D convolutional layers for feature extraction (downsampling). Before the BDA and DSA module, we both conduct the operation of **LayerNorm**. Unlike MaxViT[2] applying a standard MLP network after calculating the attention, we feed the output feature in to the FF module. Finally the Feature up sample block restores the same resolution as input. To upsample the feature map, ConvTranspose3D in conducted. There are four 3D conv layers in the feature extraction part. The corresponding kernel sizes are $5 \times 5 \times 5$, $3 \times 3 \times 3$, $1 \times 1 \times 1$, and $3 \times 3 \times 3$. There are one 3D convTranspose layer and three 3D conv layers in the decoder part for upsampling. The corresponding kernel sizes are $1 \times 3 \times 3$, $3 \times 3 \times 3$, $1 \times 1 \times 1$, and $3 \times 3 \times 3$. We employ 3D-CNN layers To extract the feature map of uncertainty. All source code required for conducting and analyzing the experiments will be made publicly available upon publication of the paper.

2. Ablation Study and Experimental Results

Ablation Study: In the paper, to test the efficiency of each module, we directly remove each part of the module separately. However, we should not ignore the effect brought by the reduction of parameter count. As shown in Tab. S1, the parameter count of FF is the largest among the three parts of CMT. Hence it brings the most obvious drop.

Experimental Results: As shown in Tab. S2, all previous learning-based SOTA algorithms can not be adapted to dif-

BDA	DSA	FF	Parameter	Flops
✗	✓	✓	55M	4389G
✓	✗	✓	55M	4389G
✓	✓	✗	19M	2050G

Table S1. Computational complexity of different models.

Algorithms	Trained mask	New mask 1	New mask 2
Ours	36.52 0.985	36.51 0.985	36.53 0.985
DUN-3DUnet	35.32 0.968	31.58 0.934	31.75 0.935
BIRNAT	33.31 0.951	23.13 0.730	23.10 0.730
RevSCI	33.92 0.956	18.99 0.537	18.93 0.535

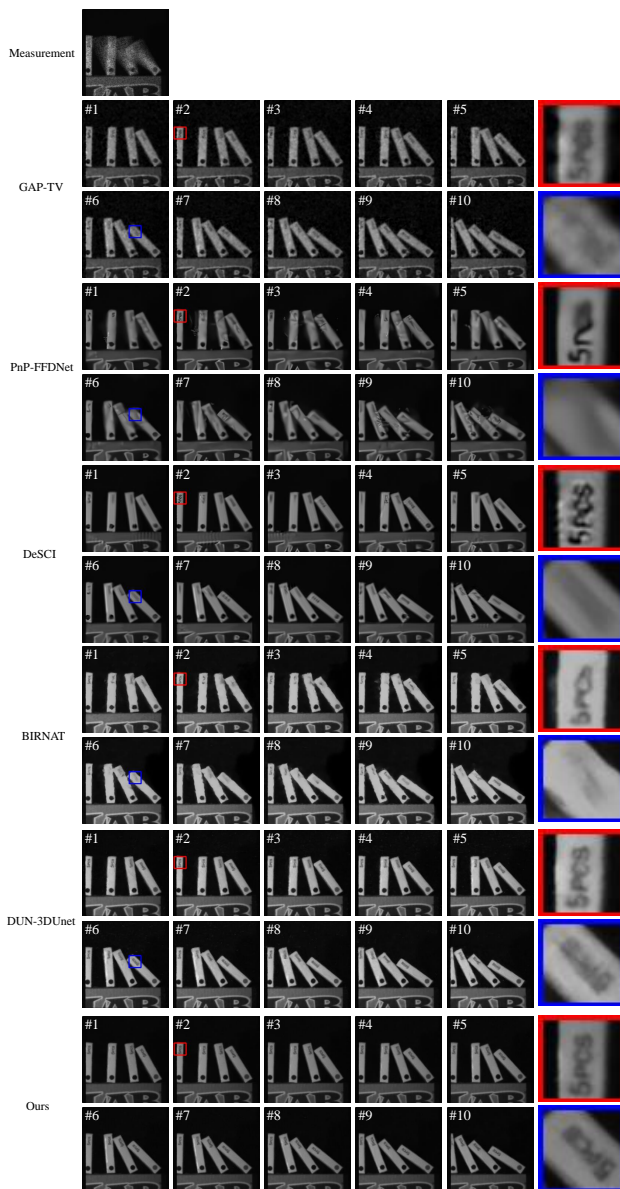
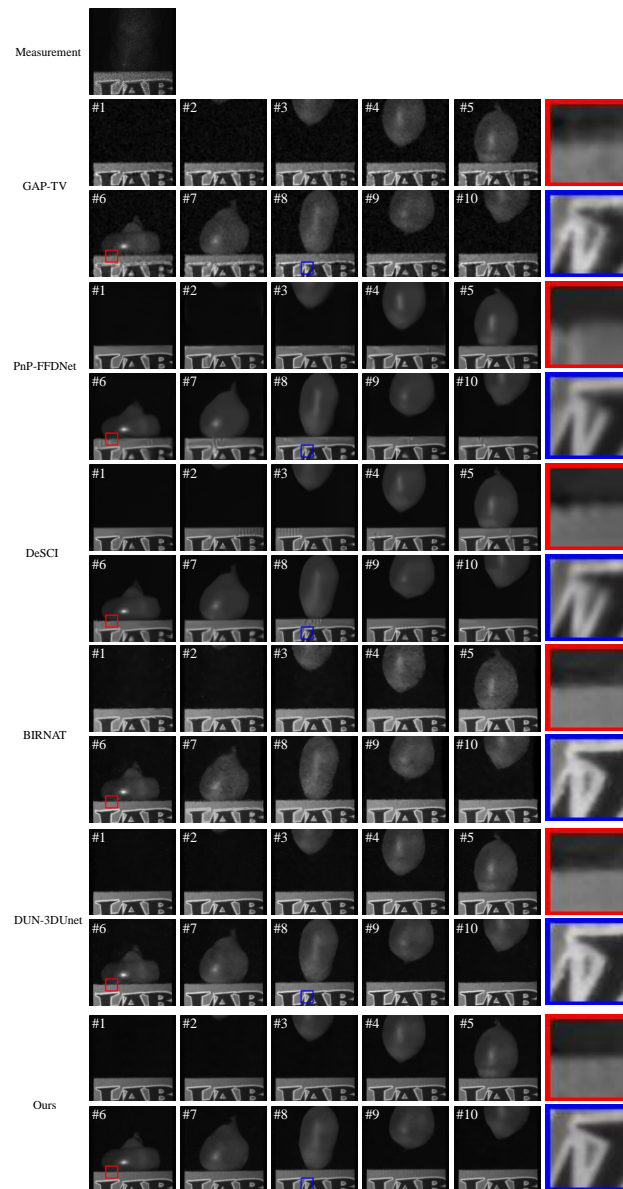
Table S2. Quantitative comparison with different masks.

ferent masks directly. Though MetaSCI claims that it can adapt to different masks, it still needs additional training. The adaptability of the algorithm greatly promotes the application of the algorithm in practical scenarios.

The measurements and all frames of the real data **Water Balloon** and **Domino** are shown in Fig. S1 and Fig. S2. We reconstruct multiple frames from the single measurement and achieve cleaner background, sharper edges, and more detail information.

3. Model for Color Video SCI

Compared to the grayscale model, the color model shares almost the same architecture. However, since the captured measurement of color video SCI system is a Bayer mosaicked measurement, we do not fuse the RF and uncertainty map into the model to avoid the unknown adverse factors. Different from previous methods such as [1, 3] which divide the measurement into four individual parts corresponding to the Bayer-filter, our proposed model directly takes the entire Bayer measurement as input and outputs the desired color videos at each stage. In addition, the output of the first stage is sent to the Bayer filter again before being fed into the next projection.

108
109
110
111
112
113
114
115153 Figure S1. All reconstruction frames of **Domino**. Zoom in for
154 better view.155
156
157
158
159
160
161153 Figure S2. All reconstruction frames of **Water Balloon**. Zoom in for
154 better view.162
163
164
165
166
167
168
169
170
171
172
173
174
175
176
177
178
179
180
181
182
183
184
185
186
187
188
189
190
191
192
193
194
195
196
197
198
199
200
201
202
203
204
205
206
207
208
209
210
211
212
213
214
215

216	References	270
217		271
218	[1] Ziheng Cheng, Bo Chen, Guanliang Liu, Hao Zhang, Ruiying	272
219	Lu, Zhengjue Wang, and Xin Yuan. Memory-efficient net-	273
220	work for large-scale video compressive sensing. In <i>Proceed-</i>	274
221	<i>ings of the IEEE/CVF Conference on Computer Vision and</i>	275
222	<i>Pattern Recognition</i> , pages 16246–16255, 2021. 1	276
223	[2] Zhengzhong Tu, Hossein Talebi, Han Zhang, Feng Yang, Pey-	277
224	man Milanfar, Alan Bovik, and Yinxiao Li. Maxvit: Multi-	278
225	axis vision transformer. <i>arXiv preprint arXiv:2204.01697</i> ,	279
226	2022. 1	280
227	[3] Xin Yuan, Patrick Llull, Xuejun Liao, Jianbo Yang, David J.	281
228	Brady, Guillermo Sapiro, and Lawrence Carin. Low-cost	282
229	compressive sensing for color video and depth. In <i>IEEE Con-</i>	283
230	<i>ference on Computer Vision and Pattern Recognition (CVPR)</i> ,	284
231	pages 3318–3325, 2014. 1	285
232		286
233		287
234		288
235		289
236		290
237		291
238		292
239		293
240		294
241		295
242		296
243		297
244		298
245		299
246		300
247		301
248		302
249		303
250		304
251		305
252		306
253		307
254		308
255		309
256		310
257		311
258		312
259		313
260		314
261		315
262		316
263		317
264		318
265		319
266		320
267		321
268		322
269		323